Nature of the continuum limit in the 2D RP^2 gauge model

S. M. Catterall
Department of Physics, Syracuse University, Syracuse, New York 13244

M. Hasenbusch
Fachbereich Physik, Humboldt-Universität zu Berlin, Invalidenstr. 110, D-10099, Berlin, Germany

R. R. Horgan
University of Cambridge, DAMTP, Silver Street, Cambridge CB3 9EW, United Kingdom

R. Renken
Department of Physics, University of Central Florida, Orlando, Florida 32816
(Received 11 February 1998; published 10 September 1998)

The RP^2 gauge model which allows interpolation between the RP^2 and O(3) spin models is studied in 2D. We use Monte Carlo renormalization techniques for blocking the mean spin-spin interaction $\langle A\rangle$ and the mean gauge field plaquette $\langle P\rangle$. The presence of the O(3) renormalized trajectory is verified and is consistent with the known three-loop β function. The first-order ''vorticity'' transition observed by Solomon *et al.* is confirmed, and the location of the terminating critical point is established. New scaling flows in $(\langle A\rangle,\langle P\rangle)$ are observed associated with a large exponent κ in the range 4–5. The scaling flows are found to give rise to a strong crossover effect between regions of high and low vorticity and are likely to induce an apparent signal for scaling in the crossover region which we propose explains the scaling observed for RP^2 and RP^3 models by Caracciolo *et al.* and also in a study of the SO(4) matrix model by Hasenbusch and Horgan. We show that the signal for this ''pseudo'' scaling will occur for the RP^2 spin model in the crossover region which is precisely the region in which computer simulations are done. We find that the RP^2 spin model is in the same universality class as the O(3) spin model, but that it is likely to require a very large correlation length before the true scaling of this class sets in. We conjecture that the scaling flows are due either to the influence of a nearby new renormalized trajectory or to the ghost of the Kosterlitz-Thouless trajectory in the associated XY model. In the former case it is argued that the ''vorticity'' fixed point controlling the critical behavior terminating the first-order line cannot be identified with the conjectured new renormalized trajectory.
[S0556-2821(98)02317-0]

PACS number(s): 11.15.Ha, 05.50.+q, 11.10.Lm, 64.60.Fr

I. INTRODUCTION

The nature of the phase diagram for two-dimensional RP^N models has been the subject of much recent discussion [1,2]. In [1], Caracciolo *et al.* compare the correlation length computed from simulation with that predicted from the perturbative β function using the exact results for the mass gap in O(N) models. They found that for RP^2 (RP^3) the observed correlation length on lattices up to $L=512$ was smaller than the expected value by a factor of 10^7 (10^4). Their conclusion was that either the asymptotic regime is indeed very far removed from the regime of their study, requiring lattices of sizes of 10^9 (10^5), or that these theories were not asymptotically free, but that there exists a phase transition at finite β (nonzero temperature). Caracciolo *et al.* indeed provide evidence for the latter scenario by showing that their data scale in a manner consistent with a Kosterlitz-Thouless parametrization. The two persuasive features are thus that the correlation length is much smaller than that expected assuming an asymptotically free theory and that scaling of the data is observed. This phenomenon occurs in a large class of models and the question is whether the signal for a phase transition at finite β and the observed scaling of data are genuine or not.

The same effects have been observed to a less extreme extent by Hasenbusch and Horgan [3] who investigated the continuum limit of the SO(4) matrix model. The measured ratio of the mass gap to $\Lambda_{\overline{\rm MS}}$, was compared with the theoretical prediction obtained using the Bethe ansatz [4]. There was a disagreement between theory and experiment by about a factor of 4, the measured correlation length being about 4 times smaller than expected. However, the measurement using the covering group was in excellent agreement with theory. The numerical method used, due to Lüscher *et al.* [5], relies in part on measuring the correlation length in a large volume and establishing that scaling holds with only small and perturbative violations. Although in the SO(4) case there were strong indications that the results scaled, the discrepancy between simulation and theory led to the conclusion that the signal for scaling was only apparent and that a true continuum limit had not been achieved in the large volume simulation. It was conjectured that the cause of the deception was the presence of vortices in the SO(4) model, which are absent in the case of the covering group, since

$$\Pi_1(\mathrm{SO}(4))=Z_2, \quad \Pi_1(\mathrm{SU}(2))=0. \tag{1.1}$$

One question is, therefore, whether a bogus signal for scaling can be observed in the presence of vortices in two dimensions. In the work presented here this question is addressed in the context of an RP^2 gauge theory which allows an inter-

polation between the pure RP^2 and O(3) spin models. This gauge model contains Z_2 vortices coupled to a chemical potential. We observe the conventional O(3) renormalized trajectory and show that our results are consistent with the known three-loop β function. We establish the existence of a first-order transition, first suggested by Solomon *et al.* [6], for which the order parameter is the vorticity. The critical point terminating this first-order line will be in the domain of a new ''vorticity'' fixed point. Using Monte Carlo renormalization group (MCRG) techniques, we observe certain flows on which the blocked observables scale and suggest that these scaling flows are due to the influence of a nearby renormalized trajectory which gives rise to the possibility of the existence of a fixed point other than the O(3) one. We argue that it is unlikely that any new fixed point can be identified with the inferred ''vorticity'' fixed point. Our results strongly indicate that the apparent or ''pseudo'' scaling behavior is due to a crossover effect associated with the proximity of the new scaling flows to the line of RP^2 spin models in coupling constant space. The crossover is between regions of high and low vorticity, which emphasizes the crucial role of vorticity in the observed properties of the model. Where relevant, our results confirm or complement those obtained by Solomon *et al.* [6] in an earlier study of this model.

Another reason for studying the RP^2 gauge models is that it has been conjectured [2] that in 2D the continuum limit in the RP^2 spin model is distinct from that in the O(3) spin model. Niedermayer *et al.* [7] and Hasenbusch [8] have suggested that this conjecture is incorrect and that there does exist a continuum limit in the RP^2 model which is controlled by the O(3) fixed point. The essential question is whether or not the RP^2 model is in the same universality class as the O(3) model. By using MCRG methods to show the topology of renormalization group trajectories in the RP^2 gauge theory, we find that a consistent and simple interpretation of our results is that the RP^2 and O(3) models are in the same universality class: an interpretation which supports the conclusions of Niedermayer *et al.* [7] and Hasenbusch [8].

All results are for RP^2 gauge models, but the simulation can be generalized to RP^{N-1} and a cursory investigation for $N>3$ has indicated that broadly similar results hold for this general case.

In Sec. II we define the model under study, in Sec. III we briefly describe the simulation techniques, in Sec. IV we define the Monte Carlo renormalization group method used and describe the measurement procedure, in Sec. V we present the results, in Sec. VI we give a discussion, and in Sec. VII we draw our conclusions.

II. MODEL

The action used is

$$S(\{\mathbf{S}\},\{\sigma\}) = -\beta\left(\sum_{\mathbf{x},\boldsymbol{\mu}} \mathbf{S}_x \cdot \mathbf{S}_{\mathbf{x}+\boldsymbol{\mu}} \sigma_{\mathbf{x},\boldsymbol{\mu}} + \mu \sum_{\mathbf{x}} P_{\mathbf{x}}(\sigma) \right), \tag{2.1}$$

where $\mathbf{x}=(x_1,x_2)$, $x_1, x_2 \in Z$, $1 \leqslant x_1, x_2 \leqslant L$, labels the sites of an integer 2D square lattice of side L, and $\boldsymbol{\mu}$ takes values in $\boldsymbol{\mu}_1=(0,1)$, $\boldsymbol{\mu}_2=(1,0)$. The spin $\mathbf{S}_\mathbf{x}$ is a unit length three-component vector at site $\mathbf{x}$ and $\sigma_{\mathbf{x},\boldsymbol{\mu}}$ is a gauge field on the link $(\mathbf{x},\boldsymbol{\mu})$ taking values in $[1,-1]$. The plaquette of gauge fields is denoted by $P_\mathbf{x}(\sigma)$ where

$$P_\mathbf{x}(\sigma) = \sigma_{\mathbf{x},\boldsymbol{\mu}_1} \sigma_{\mathbf{x}+\boldsymbol{\mu}_1,\boldsymbol{\mu}_2} \sigma_{\mathbf{x}+\boldsymbol{\mu}_2,\boldsymbol{\mu}_1} \sigma_{\mathbf{x},\boldsymbol{\mu}_2}. \tag{2.2}$$

This action is invariant under the gauge transformation

$$\mathbf{S}_\mathbf{x} \rightarrow g_\mathbf{x} \mathbf{S}_\mathbf{x},$$
$$\sigma_{\mathbf{x},\boldsymbol{\mu}} \rightarrow g_\mathbf{x} \sigma_{\mathbf{x},\boldsymbol{\mu}} g_{\mathbf{x}+\boldsymbol{\mu}}, \tag{2.3}$$

with $g_\mathbf{x} \in [1,-1]$.

Vortices reside on plaquettes where $P_\mathbf{x}(\sigma)=-1$ and are suppressed (enhanced) if the chemical potential μ is positive (negative). The pure O(3) model corresponds to $\mu \rightarrow \infty$ and the pure RP^2 model corresponds to $\mu=0$.

III. SIMULATION

A local update was used comprising a combination of heat-bath, microcanonical, and demon schemes. For fixed gauge fields the spins $\{\mathbf{S}\}$ were first updated by a heat-bath algorithm which can be generalized to O(N), and so for this section we will consider $\mathbf{S}_\mathbf{x}$ to be an N-component spin of unit length. The heat-bath method is to project each spin onto a 3D subspace of the N-dimensional space in which the spins take their values. The 3D subspace is chosen at random, but is the same for all spins during one lattice update. Let the projection of $\mathbf{S}_\mathbf{x}$ onto this space be denoted $\mathbf{R}_\mathbf{x}$. Then clearly

$$(\mathbf{R}_\mathbf{x})_i = (\mathbf{S}_\mathbf{x})_{j_i}, \quad i=1,2,3, \quad 1 \leqslant j_1 < j_2 < j_3 \leqslant N, \tag{3.1}$$

where the j_i are chosen randomly subject to the restrictions above. The single-site probability distribution for $\mathbf{R}_\mathbf{x}$ is then

$$Q(\mathbf{R}_\mathbf{x}) \propto \exp(\mathbf{M}_\mathbf{x} \cdot \mathbf{R}_\mathbf{x}), \tag{3.2}$$

where

$$\mathbf{M}_\mathbf{x} = \beta \sum_{\boldsymbol{\mu}} \left(\mathbf{R}_{\mathbf{x}+\boldsymbol{\mu}} \sigma_{\mathbf{x},\boldsymbol{\mu}} + \mathbf{R}_{\mathbf{x}-\boldsymbol{\mu}} \sigma_{\mathbf{x}-\boldsymbol{\mu},\boldsymbol{\mu}} \right). \tag{3.3}$$

The heat-bath update of the spin configuration $\{\mathbf{S}\} \rightarrow \{\mathbf{S}'\}$ is done successively at each site by replacing $\mathbf{R}_\mathbf{x}$ by $\mathbf{R}'_\mathbf{x}$ chosen from the distribution $Q(\mathbf{R}'_\mathbf{x})$ and making the assignment

$$(\mathbf{S}'_\mathbf{x})_{j_i} = (\mathbf{R}'_\mathbf{x})_i, \quad i=1,2,3,$$
$$(\mathbf{S}'_\mathbf{x})_k = (\mathbf{S}_\mathbf{x})_k, \quad \forall k \neq j_1, j_2, j_3. \tag{3.4}$$

The microcanonical spin update $\{\mathbf{S}\} \rightarrow \{\mathbf{S}'\}$ is also done successively at each site and is given by the replacement

$$\mathbf{S}_\mathbf{x} \rightarrow \mathbf{S}'_\mathbf{x} = -\mathbf{S}_\mathbf{x} + \frac{2(\mathbf{S}_\mathbf{x} \cdot \mathbf{M}_\mathbf{x}) \mathbf{M}_\mathbf{x}}{|\mathbf{M}_\mathbf{x}|^2}. \tag{3.5}$$

The demon update is applied to the gauge fields only. In general, it is only necessary to introduce one demon variable for the whole gauge configuration. However, when running on a massively parallel computer, it is necessary to have one demon per processor and then each demon must migrate through the whole lattice. This is easily achieved by moving

demons sequentially between processors. We illustrate the method with one demon variable d, $d \geqslant 0$. The action in Eq. (2.1) is augmented by the demon to become

$$S_{\rm demon}(\{\mathbf{S}\},\{\sigma\},d) = S(\{\mathbf{S}\},\{\sigma\}) + \beta d. \tag{3.6}$$

Then for each link $(\mathbf{x},\boldsymbol{\mu})$ the trial gauge field update is $(\sigma_{\mathbf{x},\boldsymbol{\mu}},d) \rightarrow (-\sigma_{\mathbf{x},\boldsymbol{\mu}},d')$, where d' is chosen so that $S_{\rm demon}$ is unchanged. That is,

$$d' = d - 2\sigma_{\mathbf{x},\boldsymbol{\mu}}\{\mathbf{S}_{\mathbf{x}}\cdot\mathbf{S}_{\mathbf{x}+\boldsymbol{\mu}} + \mu(\sigma_{\mathbf{x},\boldsymbol{\nu}}\sigma_{\mathbf{x}+\boldsymbol{\nu},\boldsymbol{\mu}}\sigma_{\mathbf{x}+\boldsymbol{\mu},\boldsymbol{\nu}} + \sigma_{\mathbf{x}-\boldsymbol{\nu},\boldsymbol{\nu}}\sigma_{\mathbf{x}-\boldsymbol{\nu},\boldsymbol{\mu}}\sigma_{\mathbf{x}-\boldsymbol{\nu}+\boldsymbol{\mu},\boldsymbol{\nu}})\}, \tag{3.7}$$

where $\boldsymbol{\nu}$ is the orthogonal vector to $\boldsymbol{\mu}$. The update is accepted only if $d' \geqslant 0$. Note that the update is microcanonical in the augmented configuration space of fields plus demon and hence it is independent of β.

One complete lattice update consisted of one heat-bath update followed by an alternating sequence of $N_{\rm MD}$ microcanonical and demon updates. The value of $N_{\rm MD}$ that optimizes the decorrelation of the configurations depends on many factors, and we did not spent much effort in tuning $N_{\rm MD}$, but regard $N_{\rm MD} \approx 10$ as a reasonable value. The heat-bath update took about 10 times the time of the combined microcanonical and demon updates, and so there was little time penalty for this choice. Depending on the coupling constant values, we found that decorrelated configurations were produced within 2–30 iterations. Lattice sizes ranged from 64^2 to 512^2, and typically the numbers of configurations per run were, e.g., 2×10^6 for 64^2 and 5×10^5 for 256^2.

The simulations were carried out on the HITACHI SR2201 computers in the Cambridge High Performance Computing Facility and in the Tokyo Computing Centre.

IV. MONTE CARLO RENORMALIZATION SCHEME

The objective is to establish the topology of renormalization group (RG) flows in the relevant large-scale variables and infer the phase structure of the model. After sufficient blocking we assume that we are dealing with renormalized observables, and so different phases will be distinguished by singularities in the renormalization group flows. This has been discussed, for example, by Nienhuis and Nauenberg [9] and by Hasenfratz and Hasenfratz [10]. We assume that there are at most two relevant couplings in the neighborhood of any fixed point in which we are interested. We also assume that the chosen blocked operators have components which span the two-dimensional space of relevant operators, i.e., the operators conjugate to these relevant couplings. From our earlier experience [3] and from the surmise stated in the introduction that vorticity plays a vital role, we chose to study how the mean values of the spin-spin interaction A and of the plaquette P flow under blocking. For a given configuration these quantities are defined by

$$A = \frac{1}{2V}\sum_{\mathbf{x},\boldsymbol{\mu}} \mathbf{S}_{\mathbf{x}}\cdot\mathbf{S}_{\mathbf{x}+\boldsymbol{\mu}}\sigma_{\mathbf{x},\boldsymbol{\mu}},$$

$$P = \frac{1}{V}\sum_{\mathbf{x}} P_{\mathbf{x}}(\sigma). \tag{4.1}$$

$\langle A\rangle$ lies in $[0,1]$ and $\langle P\rangle$ lies in $[-1,1]$, and the mean vorticity is defined by $\mathcal{V} = (1-P)/2$.

For each configuration $\{\mathbf{S},\sigma\}$ on a lattice of side L, we derive a blocked configuration $\{\mathbf{S}^B,\sigma^B\}$ on a lattice of side $L/2$. The blocking transformation for the spins is

$$\mathbf{S}^B_{\mathbf{x}_B} = \frac{\mathbf{S}_{\mathbf{x}} + \alpha(\mathbf{S}_{\mathbf{x}+\boldsymbol{\mu}_1}\sigma_{\mathbf{x},\boldsymbol{\mu}_1} + \mathbf{S}_{\mathbf{x}+\boldsymbol{\mu}_2}\sigma_{\mathbf{x},\boldsymbol{\mu}_2} + \mathbf{S}_{\mathbf{x}-\boldsymbol{\mu}_1}\sigma_{\mathbf{x}-\boldsymbol{\mu}_1,\boldsymbol{\mu}_1} + \mathbf{S}_{\mathbf{x}-\boldsymbol{\mu}_2}\sigma_{\mathbf{x}-\boldsymbol{\mu}_2,\boldsymbol{\mu}_2})}{|\text{numerator}|}. \tag{4.2}$$

Based on earlier work by Gottlob *et al.* [11], the parameter α was chosen to be 0.0625. Choosing other reasonable values for α was found not to change any outcome or conclusion. This gauge-invariant blocking transformation is shown in Fig. 1.

To block the gauge field the products of gauge fields were computed for the three Wilson lines joining the end points of the blocked link shown in Fig. 1. These field products are denoted by W_0, W_+, W_-. For the blocked link joining $\mathbf{x}$ to $\mathbf{x}+2\boldsymbol{\mu}$, the W_i are given by

$$W_0 = \sigma_{\mathbf{x},\boldsymbol{\mu}}\sigma_{\mathbf{x}+\boldsymbol{\mu},\boldsymbol{\mu}},$$

$$W_+ = \sigma_{\mathbf{x},\boldsymbol{\nu}}\sigma_{\mathbf{x}+\boldsymbol{\nu},\boldsymbol{\mu}}\sigma_{\mathbf{x}+\boldsymbol{\mu}+\boldsymbol{\nu},\boldsymbol{\mu}}\sigma_{\mathbf{x}+2\boldsymbol{\mu},\boldsymbol{\nu}},$$

$$W_- = \sigma_{\mathbf{x}-\boldsymbol{\nu},\boldsymbol{\nu}}\sigma_{\mathbf{x}-\boldsymbol{\nu},\boldsymbol{\mu}}\sigma_{\mathbf{x}+\boldsymbol{\mu}-\boldsymbol{\nu},\boldsymbol{\mu}}\sigma_{\mathbf{x}+2\boldsymbol{\mu}-\boldsymbol{\nu},\boldsymbol{\nu}}, \tag{4.3}$$

where $\boldsymbol{\nu}$ is the orthogonal vector to $\boldsymbol{\mu}$. The blocked gauge field was assigned the majority sign of the W_i:

$$\sigma^B_{\mathbf{x}_B,\boldsymbol{\mu}_B} = \frac{W_+ + W_0 + W_-}{|W_+ + W_0 + W_-|}. \tag{4.4}$$

This blocking transformation has the important property that it ensures that two vortices on adjacent plaquettes of the original lattice will cancel and not survive in the blocked lattice. This is clearly true if the vortices lie in the same 2×2 block since they add mod 2, but the majority rule guarantees cancellation also when two adjacent vortices lie on either side of the block link separating two neighboring blocks. This is illustrated in Fig. 2.

This blocking scheme gives the most local blocked action for free field theory [11] and makes no *a priori* assumptions about the possible topology of the RG flows under study. To try to optimize the scheme [12,13,14] is not an option because optimization requires, by its nature, that the existence and location of fixed points and renormalized trajectories are

already known. This is not the case here. Any attempt to *a priori* tune the scheme with respect to features yet to be discovered is not possible.

For a given pair of coupling constants (β,μ) and given lattice size $L\times L$, each configuration was blocked by successive transformations until the blocked lattice size was 8×8. The operator expectations $\langle A\rangle_L(\beta,\mu)$ and $\langle P\rangle_L(\beta,\mu)$ were then measured and averaged over all configurations. For a given (β,μ) this was done for $L=64,128,256,512$, which gives four points on a segment of a flow in the $(\langle A\rangle,\langle P\rangle)$ plane with each point labelled by the initial lattice size. Each point corresponds to a rescaling of length by a factor of 2 compared with the previous point.

The errors in the observables were determined by averaging the results for successive configurations in bins of 2^M, $M=0,1,2,\ldots$, and calculating the errors on the ensemble of bin-averaged measurements [15]. The true error is the asymptotic value achieved for large enough M. The decorrelation length can also be estimated from the behavior of the error as a function of M. The number of independent configurations ranged from about 600 for $L=512$ to in excess of 2×10^4 for $L=64$. Errors were also estimated from the ensemble of independent measurements from different processors.

V. RESULTS

Each flow segment consisting of four points, but more complete flows, can be built up by extending the flow in either direction by tuning to new couplings (β',μ') so that

$$\langle A\rangle_{L'}(\beta',\mu')=\langle A\rangle_L(\beta,\mu),$$
$$\langle P\rangle_{L'}(\beta',\mu')=\langle P\rangle_L(\beta,\mu), \tag{5.1}$$

for some L and L'. The flow for a given (β',μ') can then be computed. In general, this will be an approximate procedure because a segment in the $(\langle A\rangle,\langle P\rangle)$ plane is the projection onto this plane of part of a full flow in the higher dimensional space of observables. By tuning as described we can ensure only that the projections of blocked points coincide, not the blocked points themselves. In principle, we need to match a full complement of observables by tuning a complete set of couplings, conjugate to these observables, which define the most general action consistent with the symmetry. In general, the effect of couplings which are not included cannot be properly taken into account. However, we assume that in the neighborhood of a fixed point there will be at most two relevant couplings and that the projection onto the (β,μ) plane of the space they span is nonsingular. The effect of irrelevant couplings is mitigated by performing an initial blocking by a factor which will significantly reduce the errors induced by the projection so that we are effectively dealing with renormalized operators. Since the target lattice is always 8×8, the size of this factor depends on the initial lattice size and hence on available CPU time. For our study this initial blocking factor had a minimum value of 8.

Because we always block a number of times, the operators so generated are nonlocal from the point of view of the original lattice and so represent large-scale smoothed variables. These observables on the original lattice reflect the couplings at the scale of the blocked lattice, which, after a sufficient number of blocking steps, depend on the relevant renormalized couplings only. We assume that a ''sufficient number'' is at least 3, a fact that is substantiated below by our results.

There are errors due to finite-size effects which can be parametrized in terms of the parameter $z=\xi_L/L$, where ξ_L is the correlation length on the $L\times L$ lattice. Because the target lattice is the same size throughout, the values of z associated with coinciding points, Eq. (5.1), are similar and so the mismatch in the finite-size errors between different segments joining up to make a longer flow will be minimized. There will nevertheless be a residual finite-size effect which is generally not possible to estimate except in the case of the O(3) spin model, which is discussed in the next section.

The details of the flows can depend on z and the details of the blocking scheme. It follows that conclusions about the physical properties of the theory can be deduced only from universal or topological properties of the flows such as the occurrence of fixed points and singular behavior.

A. O(3) renormalized trajectory

In the limit $\mu\to\infty$ we recover the O(3) spin model, and to test our procedures and assumptions, we should, at the very least, be able to recover the perturbative β function for this model. The projection of the O(3) renormalized trajectory onto the (β,μ) plane is the β axis. We expect corrections to scaling due to finite lattice-spacing artifacts which will be a function of L. We find that our method works well for sufficiently large β once the tree-level approximation for these scaling corrections has been taken into account. Consider the block observable $A^B=\mathbf{S}^B_{\mathbf{x}_B}\cdot\mathbf{S}^B_{\mathbf{y}_B}$ with the blocking transformation defined in Eq. (4.2). For large β we write

$$\mathbf{S}_{\mathbf{x}}=\mathbf{q}\sqrt{1-\beta^{-1}\boldsymbol{\phi}_{\mathbf{x}}^2}+\beta^{-1/2}\boldsymbol{\phi}_{\mathbf{x}}, \tag{5.2}$$

where $\mathbf{q}=(1,0,0)$ and $\boldsymbol{\phi}=(0,\phi_1,\phi_2)$. Using Eq. (4.2) and keeping terms up to β^{-1}, we find after one blocking step that

$$\mathbf{S}^B_{\mathbf{x}_B}=\mathbf{q}\sqrt{1-\beta^{-1}\boldsymbol{\Phi}^2_{\mathbf{x}_B}}+\beta^{-1/2}\boldsymbol{\Phi}_{\mathbf{x}_B}, \tag{5.3}$$

with

$$\boldsymbol{\Phi}_{\mathbf{x}_B}=\frac{\boldsymbol{\phi}_{\mathbf{x}}+\alpha\Sigma_{\boldsymbol{\mu}}\phi_{\mathbf{x}+\boldsymbol{\mu}}}{1+4\alpha}, \tag{5.4}$$

and where $\boldsymbol{\mu}$ is summed over nearest neighbor links. For large β we expect the blocked expectation value $\langle A\rangle_L$ on the 8×8 lattice to behave as

$$\langle A\rangle_L=1-C(L)/\beta+O(1/\beta^2). \tag{5.5}$$

For large enough L we expect $C(L)$ to attain its limiting value. However, there is still some variation in $C(L)$ for the values of L we are using. In order to accommodate the bulk of this correction to scaling, we define the effective coupling $\beta_{\rm eff}$ by

$$\beta_{\rm eff}(L,\beta)=\frac{C(L)}{1-\langle A\rangle_L(\beta)} \tag{5.6}$$

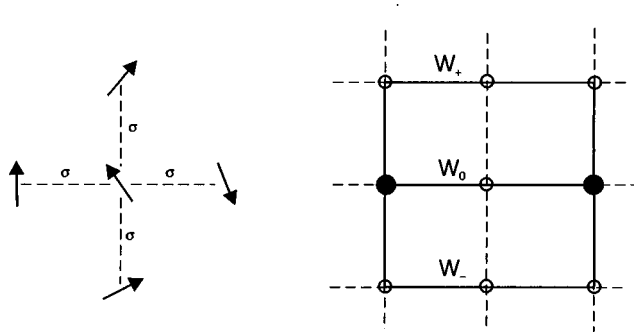

FIG. 1. Blocking strategies for spins and gauge fields. A gauge-covariant linear combination of a spin and its nearest neighbors defines the blocked spin and the gauge field on the blocked link, which connects the solid-black sites, is assigned the majority sign of the three Wilson lines W_+, W_0, W_-.

and modify the matching condition of Eq. (5.1) in this case to become

$$\beta_{\rm eff}(L,\beta)=\beta_{\rm eff}(L',\beta'). \tag{5.7}$$

We then expect that

$$\log(L/L')=\int_u^{u'}\frac{du}{\beta(u)}, \tag{5.8}$$

where $u=1/\beta$, $u'=1/\beta'$.

$C(L)$ is determined from a free field theory calculation on an L^2 lattice of the kinetic term for the blocked field $\mathbf{\Phi_x}$, which is defined on the target L_B^2 lattice by iteration of Eq. (5.4). This calculation is done easily numerically, and the results are given in Table I. We use $L_B=8$ in subsequent calculations.

Using Eq. (5.8) and the three-loop β function from [5], we determine sequences for the bare coupling β for which successive terms correspond to blocking by a factor of 2. In Table II we compare the values of $\beta_{\rm eff}$ for the two sequences $\beta=5.0$, 4.8861, 4.7721 and 2.0, 1.8803, 1.7560. If our simulation reproduces the correct β function, then the matching condition

$$\beta_{\rm eff}(2^{(m-n)}L,\beta_n)=\beta_{\rm eff}(L,\beta_m) \tag{5.9}$$

must be satisfied, where β_n is the nth term in the sequence. From Table II we see that this condition is indeed very well satisfied for the sequence starting with $\beta=5.0$. For the other sequence the larger values of $\beta_{\rm eff}$ agree well, and only as $\beta_{\rm eff}$ decreases is there an increasing discrepancy which signals a significant deviation of the three-loop approximation to the β function from the correct value and also the possible effect of the neglected L-dependent $O(1/\beta^2)$ terms in Eq. (5.6). Our expectation is confirmed that the method correctly reproduces asymptotic scaling and probes the renormalization group flow close to the renormalized trajectory.

TABLE I. The function $C(L)$ defined in Eq. (5.5) for blocking from an L^2 lattice for target lattices with $L_B=8,4$. $C(L)$ gives the tree approximation for the dependence on L/a of corrections to scaling in the O(3) spin model.

L	$C(L,L_B=8)$	$C(L,L_B=4)$
16	0.53890071	0.54363018
32	0.56795927	0.55935100
64	0.58370587	0.56866918
128	0.59303041	0.57453025
256	0.59889307	0.57829938
512	0.60266260	0.58074276

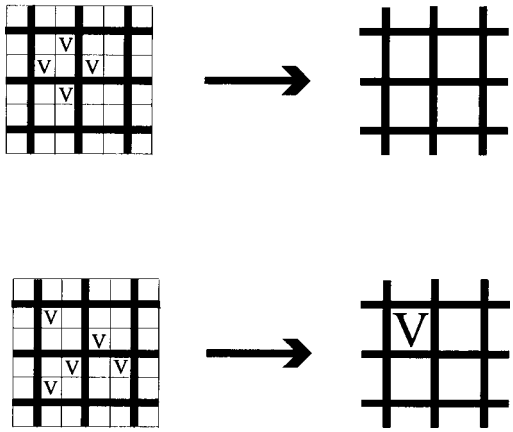

FIG. 2. The results of example blocking of two vortex configurations. Since vortices add mod 2, the blocking should yield either no blocked vortices or one blocked vortex depending on whether the original region contained an even or odd number of vortices. The majority rule of Eq. (4.4) guarantees this important property.

B. New scaling flows

In Figs. 3–9 we plot the flow segments for various (β,μ) values in the $(\langle A\rangle,\langle P\rangle)$ plane, where the longer flows in Figs. 3 and 4 are composed of superimposing segments using Eq. (5.1). There is a flow on which the observables scale. This is shown in Figs. 3 and 4. Nearby flows also showed scaling, but are not included in the figures for reasons of clarity. To see that observables scale, each flow of four points was successively overlaid using the tuning described in Eq. (5.1) with $L'=L/2$. For the scaling flows the points of

TABLE II. Values of $\beta_{\rm eff}(L,\beta)$ for sequences of bare coupling β computed using Eq. (5.8) where successive couplings in the sequence correspond to blocking by a factor of 2. The required matching condition, Eq. (5.9), for verification of asymptotic scaling is very well satisfied for the sequence at larger β, and the deviation in the other sequence is largest for the smaller values of β and is due to deviation of the three-loop approximation to the β function from the true value and possibly to terms neglected in Eq. (5.6).

	Initial lattice size L			
β	64	128	256	512
5.0		4.355(1)	4.227(3)	4.107(5)
4.8861	4.343(1)	4.244(3)	4.110(3)	3.995(5)
4.7721	4.249(1)	4.124(1)	4.002(3)	
2.0		1.2752(4)	1.1366(4)	0.9852(7)
1.8803	1.2733(2)	1.1289(4)	0.9729(7)	0.8194(4)
1.7560	1.1210(3)	0.9532(4)	0.8000(2)	

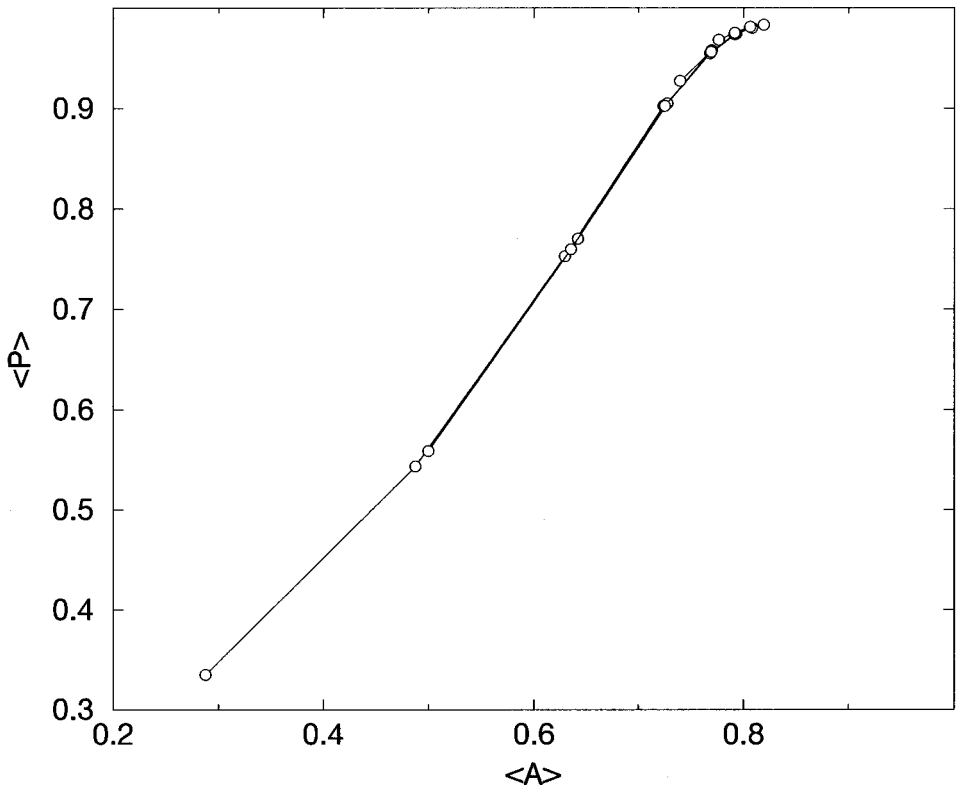

FIG. 3. The scaling flow built up from the RG flow segments of set 1 given in Table III. Each segment consists of four points corresponding to the $(\langle A\rangle,\langle P\rangle)$ values on an $L=8$ lattice blocked for given couplings from lattices with $L=64$, 128, 256, 512, respectively. The segments are adjusted so that they overlay each other, and it can be seen from this figure, and from Table III, that the points on different segments coincide very well, indicating that scaling holds. There are two errant points corresponding to the two largest β values and $L=512$.

the overlaid flow segments coincide very well within errors (the tuning is not absolutely exact), showing that there are only very small effects from the irrelevant operators. In Table III we give the values of $(\langle A\rangle,\langle P\rangle)$ for points on the segments making up two such scaling flows, labelled set 1 and set 2, together with the initial lattice sizes and coupling constant values.

The tuning described by Eq. (5.1) was done by trial and error. We tried to estimate the effect of small increments in the coupling constant values by using the method of reweighting, but this was found not to work. This was mainly because the blocked $(\langle A\rangle,\langle P\rangle)$ values were very sensitive to the initial couplings and so to use reweighting was not a realistic possibility. Also, it was found that the effect of a change in β could be partly compensated by a change in μ. This was because the Jacobian $\partial(\langle A\rangle,\langle P\rangle)/\partial(\beta,\mu)$ was relatively small and presumably a better choice for the pair of observables and/or initial couplings would increase its value. However, in no case was this Jacobian dangerously small and tuning by trial was effective.

For these flows we did not apply a compensation for scaling corrections of the kind used in the previous section for the O(3) model. It is not possible to carry out a similar tree-level calculation to determine the compensation, if any, as a function of L/a since the model and the appropriate coupling(s) associated with the scaling flows are not known. Also, the data presented in this section were obtained before the details of the O(3) analysis were known and the possible residual dependency on L analyzed. It could be suggested that an optimized RG scheme [12,13,14] would eliminate these minor deviations, but there are impediments to the implementation of such a strategy. As discussed more fully later, it is unclear that there actually exists a fixed point associated with these flows, and even if there is, we argue that no point in the (β,μ) plane can be in its domain of attraction. Consequently, not even a singular blocking scheme can move the supposed fixed point so that the corresponding fixed point theory is in the class of models we are studying. A similar argument excludes any possibility of developing an improved action associated with the scaling flows. In order to do so we need to establish the existence, nature, and position of the fixed point—information we do not have. Overall, the deviation from scaling for the scaling flows is not large, and we must allow for the possibility that it may be due, in some measure, to finite lattice-spacing artifacts of the kind analyzed for O(3). However, there are a few points shown which do deviate substantially from scaling for which such an explanation is unlikely. For both sets these points are for the two largest values used for β and for the largest initial lattice size $L=512$. We defer a discussion of the reasons why they do not scale well until Sec. VI.

The couplings which generate the scaling flow denoted by set 1 correspond to points on the flow separated by a blocking factor of 2. A plot of $\exp(-\mu)$ versus $g=1/\beta$ for these points can be approximated by a straight line with all except the one with smallest β well fitted by

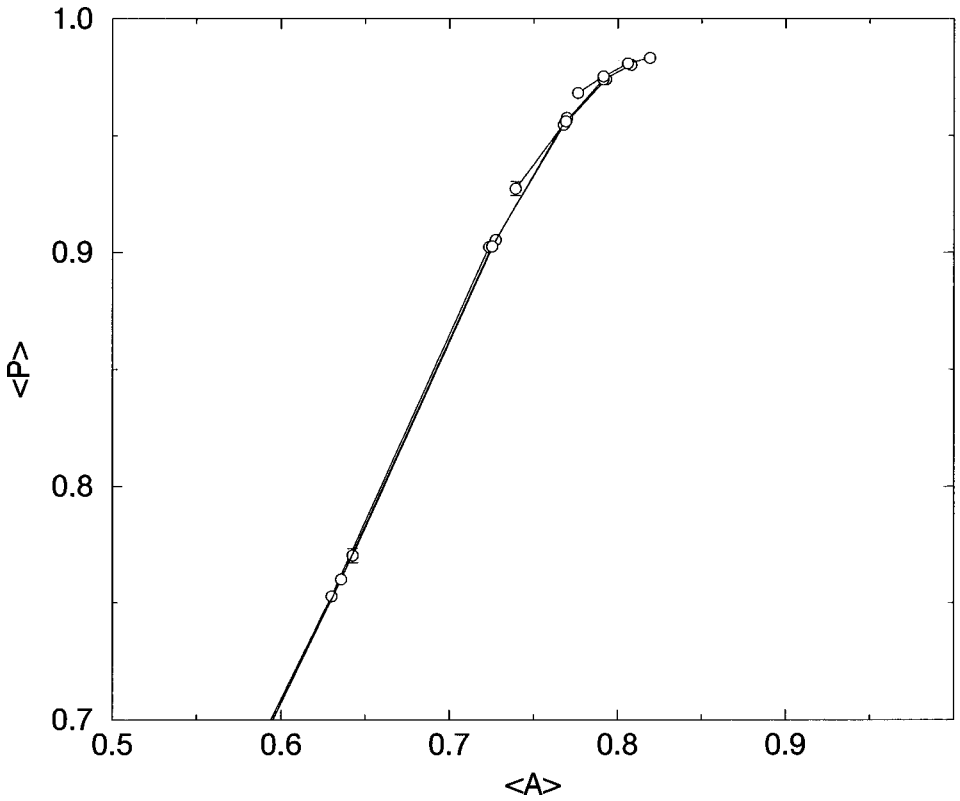

FIG. 4. Detail of Fig. 3. Caption as for Fig. 3.

$$\exp(-\mu) = 1.74(1) - 2.98(4)g. \tag{5.10}$$

This form is motivated by plots shown in Solomon *et al.* [6] where certainly the position of the first-order transition at zero temperature ($g=0$) is most easily expressed in terms of g and $\exp(-\mu)$. Phenomenologically, we find that it is consistent to associate a scaling exponent κ with the scaling flow using the relation

$$\frac{(g_1 - g^*)}{(g_2 - g^*)} = b^\kappa, \quad b = 2^p, \tag{5.11}$$

where the number of blockings for g_1 and g_2 differs by p (a factor of 2^p in change of scale) in order for the corresponding points in the $(\langle A\rangle, \langle P\rangle)$ plane to coincide on the scaling flow. This behavior is expected for g close to g^* if an infrared fixed point g^* exists. The value of g^* is a free parameter which is chosen to obtain the best fit assuming κ in Eq. (5.11) is constant. Even so, g^* is not very well determined by this alone and we find a range of values $g^* \approx 0.13 - 0.15$ to be acceptable, for which the various pairings of couplings for set 1 from Table III give the values for κ shown in Table IV. The values of μ^* in Table IV are inferred using the linear fit of Eq. (5.10). Note that the possible values of μ^* in Table IV are far removed from the value $\mu=0$ which characterizes the RP^2 model. Taking κ in the range 4–5, the dimension of the relevant operator associated with the scaling flows is

$$\Delta = D - 1/\kappa \approx 1.75 - 1.8. \tag{5.12}$$

A word of caution. The definition of κ used in Eq. (5.11) is appropriate for conventional second-order behavior. However, the consistency of the fit should be taken only as a phenomenological parametrization and it is likely that a different scaling form such as derived from Kosterlitz-Thouless (KT) behavior would give an equally good fit. For example, in [16] Seiler *et al.* study the $Z(10)$ model in 2D which they presume has a KT transition. They find that both second-order and KT scaling forms give equally good fits near the transition and that, indeed, the KT form is hard to reconcile with conventional theory.

C. First-order transition

Solomon *et al.* [6] use simple arguments to suggest that a line of first-order transitions occurs in the range $\mu_1 < \mu(\beta) < \mu_2$, $\mu_1 = -0.293$, $\mu_2 \approx -0.26$. This line of transitions will terminate in a critical point associated with a continuous transition, implying that a critical surface intersects the (β,μ) coupling constant plane. Confirmation of the first-order transition is shown in Figs. 5 and 6 where, respectively, the values of $\langle A\rangle$ and $\langle P\rangle$ for a lattice of $L=128$ are shown plotted against μ for fixed $\beta = 6.0, 7.0, 7.5, 8.0$. It is clear that there is no transition for $\beta = 6.0, 7.0$, but that there is likely to be a first-order transition for $\beta = 7.5, 8.0$. This places the critical point in the range $7.0 < \beta^* < 7.5$, which is consistent with the investigation of Solomon *et al.* [6]. The value of μ^* varies a little, but is close to -0.26. There is no detectable dependence on L, and studies on lattices with $L=256$ and $L=512$ have shown identical results within statistical errors. From Fig. 5 we infer that a good order parameter distinguishing the two phases is the vorticity. There is also a discontinuity in $\langle A\rangle$ shown in Fig. 6 which is, however, not independent of the discontinuity in $\langle P\rangle$. The value of $\langle A\rangle$ will vary rapidly since it is sensitive to, and thus reflects, the discontinuous change in the vorticity. The effective potential will

TABLE III. Values of the blocked observables $(\langle A\rangle,\langle P\rangle)$ for the flow segments constituting two neighboring scaling flows labelled by set 1 and set 2. The values of the couplings (β,μ) labelling each segment are given and the different points on a given segment are labelled by the initial lattice size L. The blocked observables were measured after blocking to a fixed target lattice size of 8×8. Scaling of the blocked observables can be seen to hold extremely well for each set by noting that the $(\langle A\rangle,\langle P\rangle)$ values lying on any given diagonal sloping from bottom left to top right agree very closely indeed, except for the largest two values of β for $L=512$. Set 1 is shown in Figs. 3 and 4.

		Initial lattice size, L			
	(β,μ)	64	128	256	512
Set 1	4.26, −0.045	0.81894(3) 0.98330(4)	0.80587(9) 0.9809(2)	0.7913(2) 0.9753(3)	0.7761(3) 0.9684(8)
	4.0, 0.0	0.80793(3) 0.98021(6)	0.7913(2) 0.9740(3)	0.7690(2) 0.9561(4)	0.739(1) 0.927(3)
	3.72, 0.06	0.79261(5) 0.97402(9)	0.7678(1) 0.9547(2)	0.7273(4) 0.9053(8)	0.6424(8) 0.770(3)
	3.45, 0.125	0.76947(6) 0.9576(1)	0.7251(2) 0.9025(4)	0.6363(4) 0.7601(10)	0.4995(6) 0.558(1)
	3.18, 0.187	0.7233(2) 0.9025(4)	0.6298(2) 0.7528(4)	0.4872(2) 0.5430(4)	0.2878(5) 0.3348(5)
Set 2	4.00, 0.02	0.81574(3) 0.98787(5)	0.80228(6) 0.9849(1)	0.7871(2) 0.9782(4)	0.7694(9) 0.967(2)
	3.73, 0.0833	0.80236(4) 0.98518(6)	0.7846(1) 0.9768(2)	0.7611(2) 0.9571(5)	0.720(1) 0.905(3)
	3.495, 0.14	0.78475(7) 0.9769(1)	0.7577(1) 0.9538(3)	0.7085(3) 0.8865(7)	0.611(2) 0.727(3)
	3.3, 0.18	0.7596(1) 0.9544(2)	0.7070(1) 0.8826(3)	0.6062(4) 0.7178(8)	0.4564(7) 0.506(1)
	3.06, 0.23	0.7050(3) 0.8821(7)	0.6002(3) 0.7105(7)	0.448(5) 0.4990(9)	0.2383(2) 0.2973(4)

show no discontinuity, and it is crude but reasonable to suppose that one particular linear combination of A and P plays this role. In Fig. 7 we plot $\langle P\rangle$ against $\langle A\rangle$, and indeed it can be seen that there is no sign of a sharp discontinuity and that the locus of points is reasonably linear. The outcome is that the combined operator

$$U_C(\mathbf{x})=\sum_{\boldsymbol{\mu}} \mathbf{S}_{\mathbf{x}}\cdot\mathbf{S}_{\mathbf{x}+\boldsymbol{\mu}}\sigma_{\mathbf{x},\boldsymbol{\mu}}+\gamma P_{\mathbf{x}}(\sigma), \tag{5.13}$$

with $\gamma\approx -0.29$, has a continuous expectation value across the transition. The orthogonal combination $U_D(\mathbf{x})$ has a discontinuous expectation value which is sensitive to the vorticity and is a good order parameter. The simple and persuasive argument of Solomon *et al.* [6] is based on minimizing the energy at $\beta=\infty$ to show that a first-order transition occurs in $\langle P\rangle$ at $\mu(\infty)=1/\sqrt{2}-1$. The argument also depends on continuity of the energy, which, at $\beta=\infty$, means that $U_C(\mathbf{x})$ is identified with the local energy operator. This will be only approximate for $\beta<\infty$.

That the transition is first order should be confirmed by investigating the L dependence of the order parameter $\langle U_D\rangle$, which we have not yet done due to pressure of computer

TABLE IV. The scaling exponent κ calculated using Eq. (5.11) and various pairings of couplings $g=1/\beta$ from set 1 given in Table III. Two different choices for (g^*,μ^*) are used which correspond to the range giving consistent results for κ.

(g^*,μ^*)	Scaling exponent κ									
0.13, −0.305	5.10	4.92	4.919	4.90	4.76	4.83	4.84	4.91	4.88	4.84
0.15, −0.261	4.19	4.10	4.15	4.18	4.02	4.13	4.18	4.25	4.26	4.28

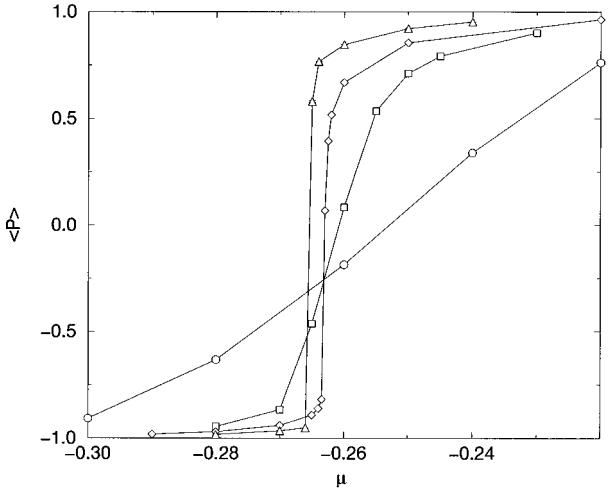

FIG. 5. $\langle P\rangle$ defined by Eq. (4.1) as a function of μ for $\beta=6.0$ (○), 7.0 (□), 7.5 (◇), and 8.0 (△).

time. However, the results in Figs. 5 and 6 convincingly demonstrate the expected discontinuity on the largest lattices.

The critical point terminating the first-order line will be in the domain of a fixed point, the ''vorticity'' fixed point, with a renormalized trajectory on which the vortex density scales, thus defining a new continuum theory with nonzero vortex density.

D. Crossover of flows

In Figs. 8 and 9 there are two further sets of flow segments, sets 3 and 4, which each show a clear crossover as a function of initial couplings. Set 3 lies to the left of set 4. These two sets are examples of the crossover effect which we infer occurs in a narrow region formed by the neighborhood of a continuous line of theories in the (β,μ) plane.

The couplings associated with sets 3 and 4 are listed in Table V where, for each set, the couplings reading from left

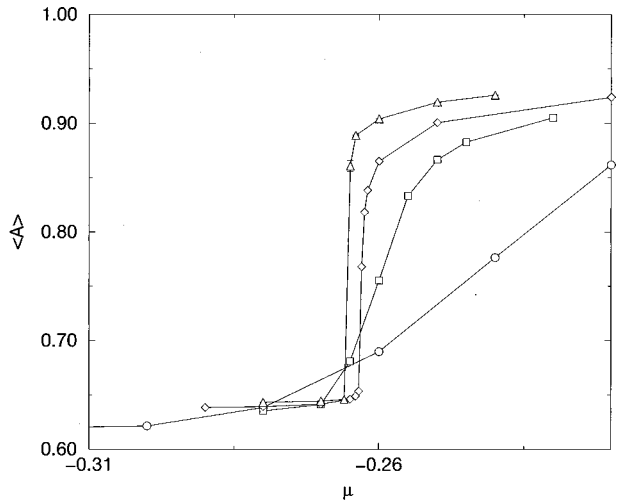

FIG. 6. $\langle A\rangle$ defined by Eq. (4.1) as a function of μ for $\beta=6.0$ (○), 7.0 (□), 7.5 (◇), and 8.0 (△).

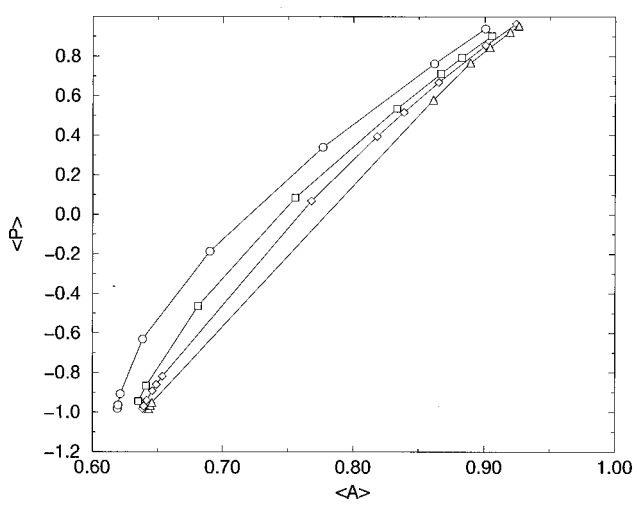

FIG. 7. $\langle A\rangle$ versus $\langle P\rangle$, defined by Eq. (4.1), for $\beta=6.0$ (○), 7.0 (□), 7.5 (◇), and 8.0 (△).

to right label the segments in order from the lowest in the figure (lowest $\langle P\rangle$) to the highest (highest $\langle P\rangle$).

We concentrate in particular on the flow segments of set 4, which correspond to the RP^2 spin model ($\mu=0$). These segments are shown for various β in the range 3.9–4.5 where the crossover in the flows is very strongly marked, occurring between $\beta=4.17$ and $\beta=4.19$. The values of $(\langle A\rangle,\langle P\rangle)$ blocked from $L=64\rightarrow L=8$ show little variation in values, but when blocked from larger L, the variation is very strong indeed. Moreover, it is clear that for $\beta=3.9-4.1$ the flow is dominated by the proximity of the scaling flows, represented

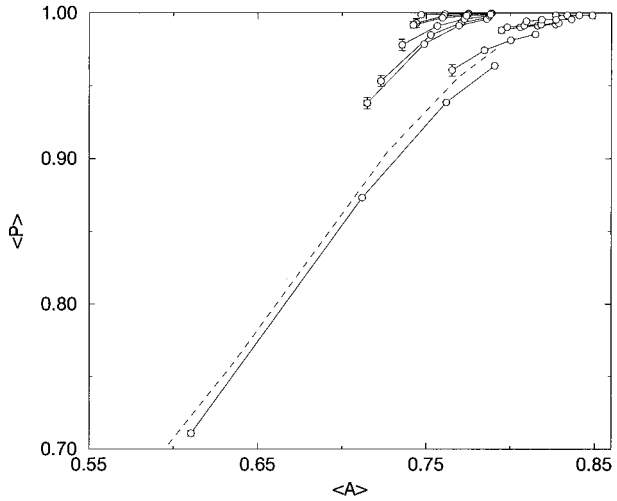

FIG. 8. Two examples sets of flows, sets 3 and 4, showing the crossover of flows. Set 3 lies to the left of set 4, and the (β,μ) values corresponding to these sets are given in Table V. Set 4 is for various β in the RP^2 model ($\mu=0$) in the range $\beta=3.9-4.5$. There is rapid variation in the renormalized $(\langle A\rangle,\langle P\rangle)$ values for small changes in β, indicating a narrow crossover from a region of high to low renormalized vorticity. For $\beta\sim 4$ the RP^2 flows closely follow the scaling flow of Fig. 3, shown here as the dashed curve, implying scaling will apparently hold until, for larger β, the crossover occurs.

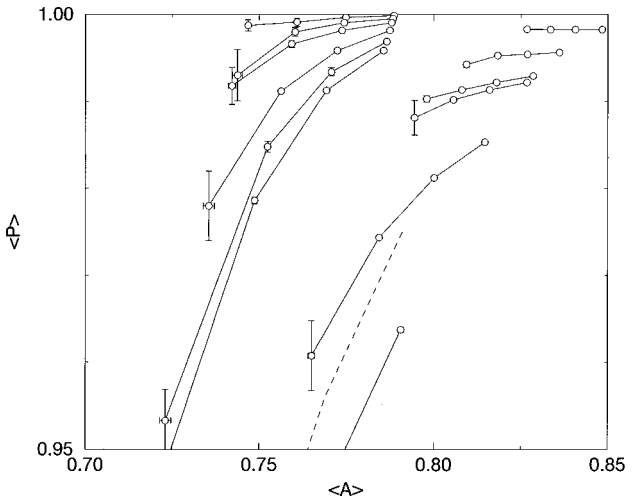

FIG. 9. Detail of Fig. 8. Caption as for Fig. 8.

as the dashed line in Figs. 8 and 9, which will induce a signal for scaling in pure RP^2 when $\beta \sim 4$. However, as β is increased, there is a strong crossover effect, and for $\beta > 4.25$, the flow is consistent with dominance by the renormalized trajectory associated with the asymptotically free O(3) fixed point at $(\beta^*, \mu^*) = (\infty, \infty)$. Consequently, the apparent scaling signal will only be transitory. For finite β there will always be some free vortices, but for $\beta > \beta_{\text{crossover}}$, we expect that the density of free vortices will vanish faster than $1/\xi^2$ and the vortex density will not scale. This behavior is consistent with the absence of a phase transition at finite β as well as with the O(3) type continuum limit in RP^2.

VI. DISCUSSION

The observation of the scaling flows reported in Sec. V B poses the question of whether we can attribute them to the influence of a nearby renormalized trajectory and so infer the existence of a new fixed point. One interpretation of the evidence for scaling is that a new renormalized trajectory exists with exponent $\kappa \approx 4-5$ and that a new fixed point lies somewhere in the complete space of coupling constants with projection onto the (β,μ) plane of $(\beta^* \approx 7,\ \mu^* \approx -0.28)$. Evidence presented in Sec. V C shows that there is also a ''vorticity'' fixed point associated with the ''vorticity'' critical point located at about $(\beta_c \approx 7,\ \mu_c \approx -0.26)$ which terminates the first-order line. Because of the proximity of these

TABLE V. The couplings associated with sets 3 and 4. For each set, the couplings reading from left to right label the segments in order from the lowest in the figure (lowest $\langle P \rangle$) to the highest (highest $\langle P \rangle$).

	(β,μ)					
Set 3	3.3 0.34	3.3 0.36	3.3 0.40	3.3 0.45	3.3 0.50	3.3 0.60
Set 4	3.9 0.0	4.05 0.0	4.17 0.0	4.19 0.0	4.29 0.0	4.5 0.0

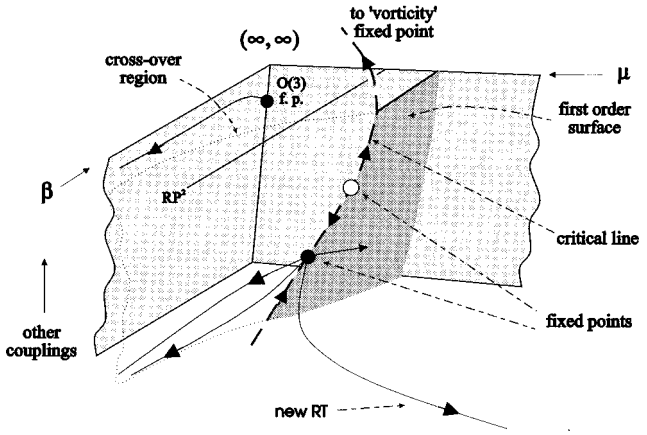

FIG. 10. An artist's impression of the RG flows consistent with the simulation results. The O(3) fixed point controls the continuum limit of RP^2 $(\mu = 0)$ and neighboring theories. A line of critical points terminates the first-order surface and defines new continuum limits characterized by nonzero continuum vorticity. The observed renormalized trajectory is shown associated with a new infrared fixed point in the critical surface (solid circle). There are cogent arguments that this fixed point does not control the second-order transition terminating the observed first-order line in the (β,μ) plane. The scenario presented here is consistent with this view, and an ultraviolet fixed point (open circle) separates the two domains of attraction shown. The crossover region is the neighborhood of the surface shown with dotted outline.

two points to each other, it is tempting to identify the new fixed point with the ''vorticity'' fixed point. However, there is no direct evidence that this is so and there are arguments against such an identification. The first is that we would expect the continuum limit defined at the ''vorticity'' fixed point to be Ising-like since the order parameter is based on a locally discrete variable: the plaquette operator $P_{\mathbf{x}}(\sigma)$. The exponent κ for Ising-like critical points is $\kappa = 8/15$, whereas for the new renormalized trajectory we find $\kappa \approx 4-5$. This is clearly inconsistent with the proposal. The second argument is that the identification of the two fixed points means that the ''vorticity'' critical point is in the domain of attraction of the new fixed point. The consequence is that there must be a fixed point of the flows in the $(\langle A \rangle, \langle P \rangle)$ plane in the limit that the initial lattice size is large enough: $L \to \infty$. This is true because flows that have bare couplings held at the critical point values must be in the critical surface and so flow towards the new fixed point. In turn, this implies that the correlation length $\xi_A(\beta,\mu)$ for a state interpolated by A must diverge at the ''vorticity'' critical point (β_c, μ_c). This is unlikely since we expect $\xi_A(\beta,\mu)$ to be bounded from above by the correlation length in the O(3) model at the same β, namely, $\xi_A(\beta,\infty)$. This is because for $\mu < \infty$ the presence of vortices introduces disorder in the system which acts to reduce the correlation length at fixed β. However, $\xi_A(\beta,\infty)$ diverges only in the limit $\beta \to 0$, the O(3) fixed point, and hence $\xi_A(\beta,\mu)$ cannot diverge at (β_c, μ_c), contradicting the proposed identification of the two fixed points. Although we did not carry out an exhaustive investigation, we found no evidence for a fixed point of the $(\langle A \rangle, \langle P \rangle)$ flows from the simulations described in Sec. V B.

In Fig. 10 we shown an artist's impression of a possible topology of the RG flows in coupling constant space consistent with this interpretation and with the results presented in Sec. V. The two axes associated with the couplings (β,μ) are augmented by a third which represents all other couplings. There are three fixed points shown. One is the usual asymptotically free O(3) infrared fixed point, and another is the new infrared fixed point we have identified in this work, both shown as solid circles. The ''vorticity'' fixed point is not shown, but its domain of attraction is separated from that of the new fixed point by an ultraviolet fixed point (open circle). The critical surface bounds the surface of first-order transitions, and the two phases associated with this transition are distinguished by the vortex density being large in one phase and small in the other. The line of intersection of the first-order surface with the (β,μ) plane is the line of first-order transitions reported above. There are a number of possible continuum limits in this model, each identified with a different fixed point. A nonzero vortex density will be associated with the continuum limit taken at the critical point controlled by the ''vorticity'' fixed point. At the new fixed point there are two relevant directions, but we cannot be sure what the relevant observables are since in this scenario the action must be augmented by other couplings so that it can be tuned to lie in the critical surface and in the domain of attraction of this fixed point. However, the presence of this renormalized trajectory dominates all flows in its neighborhood, and its influence will only be diminished if points in the critical surface are approached which are not in its domain of attraction. The example scenario of Fig. 10 is complicated, but we have found no simpler topology consistent with the results if we demand that the scaling flows are due to a nearby renormalized trajectory in an extended model.

A different interpretation is that the scaling flows are due to the ghost of the Kosterlitz-Thouless renormalized trajectory in the equivalent O(2), or *XY*, model. A cogent argument against a Kosterlitz-Thouless fixed point occurring in non-Abelian models has been given by Hasenbusch in [8], but it was conjectured in [3] that some remnant of Kosterlitz-Thouless behavior might nevertheless survive in models of this kind and give rise to the pseudoscaling behavior reported in [3]. As remarked in Sec. V B, the fit to the exponent κ using Eq. (5.11) should not be taken to rule out KT behavior in favour of conventional second-order behavior. Indeed, the large value for κ mitigates in favor of a KT interpretation [17]. This explanation has the virtue of simplicity over the alternative picture above, but it is unclear how to describe the mechanism more fully.

The deviation from scaling for the large β points for $L=512$ in sets 1 and 2 (Table III) can be explained by noting that there is no fixed point for the $(\langle A\rangle,\langle P\rangle)$ flows, and so the attempt to follow the scaling flow to larger β and into a fixed point will fail as the critical surface is approached. The conjectured renormalized trajectory dominates by virtue of its large exponent, but scaling will eventually be violated as β increases towards $\beta\sim 7$.

It is not feasible to use either an optimized blocking scheme or an improved action to elucidate the details of the scaling flows or to improve the matching. It is not established that a fixed point actually exists, and so any attempt at either approach would be premature. In any case, it is not possible for any conjectured fixed point to be ''moved'' out of its domain of attraction into the (β,μ) plane, and so the choice of operators of an optimized scheme is unclear and the choice of a simple fixed point action is unclear. Perturbation theory cannot be used to improve the action, and unlike in many successful applications of the perfect action idea, this suggested new fixed point theory is very unlikely to be asymptotically free.

The strong influence of the scaling flows gives rise to a crossover effect in the flows which signals the crossover from the vortex to the spin-wave regions of the phase diagram. For example, in pure RP^2 this occurs at about $\beta=4.18$, $\mu=0$. We would naturally associate this crossover with the observed first-order line, but it is clear that the strength of the effect is due to the nearby scaling flows. This would suggest that the first-order line and the scaling flows were related, but as argued above, a simple relationship is ruled out and it is unclear whether the proximity of the two features is a coincidence or not. The region in which the crossover occurs is quite narrow and has been shown as a surface with dotted outline in Fig. 10. As β is increased at fixed μ through this ''crossover region,'' the vorticity rapidly decreases from a high to low value especially in the neighborhood of the critical surface. This effect means that the disorder also decreases rapidly, and we would expect a corresponding rapid increase in the vector and tensor correlation lengths ξ_V and ξ_T, which are deduced, respectively, from the correlators $G_V(\mathbf{x},\mathbf{y})$ and $G_T(\mathbf{x},\mathbf{y})$ defined for RP^{N-1} by

$$G_V(\mathbf{x},\mathbf{y})=\langle \mathbf{S}_\mathbf{x}\cdot\mathbf{S}_\mathbf{y}\rangle_c\,,$$
$$G_T(\mathbf{x},\mathbf{y})=\langle[\mathbf{S}(\mathbf{x})\cdot\mathbf{S}(\mathbf{y})]^2\rangle-1/N. \tag{6.1}$$

Because G_V is not gauge invariant, it will vanish unless it is evaluated in a fixed gauge. This is analogous to the situation in QED where the electron propagator is not gauge invariant, but the pole mass is. Technically, the gauge-fixed electron propagator has a cut whose discontinuity is a gauge-dependent function of α, but whose branch point defines the gauge-invariant mass. This is due to the continuous nature of the gauge group, which does not apply in our case. A reasonable gauge choice would be to maximize $\Sigma_{\mathbf{x},\boldsymbol{\mu}}\sigma_{\mathbf{x},\boldsymbol{\mu}}$. Here G_T takes the same form as the tensor correlator defined by Caracciolo *et al.* [1] and Sokal *et al.* [2]. Because G_T is gauge invariant, it does not require gauge fixing before evaluation. When the vorticity is vanishingly small, the gauge field is equivalent to a pure gauge and can be gauge transformed to the trivial configuration $\sigma_{\mathbf{x},\boldsymbol{\mu}}=1$, $\forall\,\mathbf{x}$, $\boldsymbol{\mu}$. The physical observables in the theory are then insensitive to the chemical potential μ, and the theory is in the universality class of the O(3) fixed point.

In the O(3) continuum limit both ξ_V and ξ_T will diverge, but in the continuum limit defined by the vorticity fixed point we expect both ξ_V and ξ_T to remain finite because, as already discussed above, the presence of disorder means that they will be bounded from above, respectively, by $\xi_V(\beta,\infty)$ and $\xi_T(\beta,\infty)$, the correlation lengths at the same value of β in

the O(3) spin model. In other words, at fixed β we expect both ξ_V and ξ_T to increase as μ increases, achieving their maximum values at $\mu=\infty$ in the O(3) model. This increase could be very rapid in the vicinity of the crossover region. The operators interpolating the states in G_V and G_T are, respectively, $V_i=S_i$ and $T_{ij}=S_iS_j-1/N\delta_{ij}$. Since $\langle V_i\rangle=\langle T_{ij}\rangle=0$, they show no discontinuity across the first-order line and hence ξ_V and ξ_T will not diverge at the critical point terminating the first-order line (gauge fixing is understood where necessary). If either of ξ_V or ξ_T did diverge, it would contradict the expectation that they are bounded from above by their corresponding values in O(N) as mentioned above. In principle, we could also study $G_S(\mathbf{x},\mathbf{y})=\langle U_C(\mathbf{x})U_C(\mathbf{y})\rangle_c$ since $\langle U_C\rangle$ is continuous across the first-order line and it couples to the S-wave two-particle O(N) singlet state. The associated correlation length ξ_S should coincide with ξ_T in the continuum limit if the conventional scenario is assumed. We suggest that the divergent correlation length at the critical point is associated with the correlator of $U_D(\mathbf{x})$ or, equivalently, with the vorticity correlator

$$G_P((\mathbf{x},\mathbf{y}))=\langle P_xP_y\rangle. \tag{6.2}$$

In this study, G_P was not computed.

The pure RP^2 model ($\mu=0$) does not intersect any critical surface except the one in the basin of attraction of the O(3) fixed point at $\beta=\infty$. This confirms the conjectures of Niedermayer *et al.* [7] and Hasenbusch [8] that RP^2 and O(3) have the same continuum limit. In a simulation of pure RP^2, Kunz and Zumbach [18] observe the rapid decrease in vorticity that we have associated with the crossover region, and Niedermayer *et al.* [7] comment that in this region a sharp transition to a huge value for ξ_V is to be expected. Our result is that the crossover is very strongly marked in the renormalized quantities obtained after substantial blocking has been performed. The crossover region separates two phases, in one of which the vorticity density is high with a background of vortices pairs overlaid by a gas of free vortices, and in the other the vorticity density is low and does not scale as $\beta\rightarrow\infty$. These two phases are also separated by a first-order line, and we conjecture that a nonzero scaling limit for the vortex density could exist at the terminating critical point. Huang and Polonyi [19] have discussed the existence of a continuum limit with a nonzero scaling vorticity in a generalized 2D sine-Gordon model and the nonconservation of the kink current. A similar analysis could be fruitful in non-Abelian models of the kind discussed in this paper, although it is unclear if the same techniques are directly applicable.

In the simulation of the 2D SO(4) matrix model [3], a bogus signal for scaling was observed which led to an incorrect measurement of the $m/\Lambda_{\overline{\rm MS}}$ ratio. In the context of RP^2 we would expect a similar effect for $\beta\sim 3.9$ because in this case the model renormalizes close to the scaling flows, and so in the neighborhood of this coupling we should expect to see a good scaling signal. The effect is enhanced by the large exponent $\kappa\sim 4$ associated with these flows. Simulations which are designed to compute $m/\Lambda_{\overline{\rm MS}}$ must have $\xi_V\ll L$ for some largest practical lattice size L. Because ξ_V is rising rapidly in this region as a function of β, this means that only a small range of β is usable and that this range corresponds to theories where the vorticity is not too low since ξ_V would otherwise already be too large. The conclusion is that such simulations will see an apparent scaling due to the strong influence of the scaling flows. However, this scaling is not a signal for a continuum limit in pure RP^2, but is due to the proximity of the crossover region to the scaling flows. On much larger lattices as β is increased, a crossover to true scaling would eventually be observed: the scaling associated with the O(3) fixed point. However, this would be for prohibitively large values of ξ_V, perhaps as large as $\xi_V\sim 10^9$ [7]. We believe that this effect explains the results presented in [1], who observe scaling in RP^2 [RP^3], but who find that the observed correlation length is smaller by a factor of 10^7 [10^4] than that deduced assuming that the theory is asymptotically free. We suggest that this study is actually in the crossover regime where the correlation length is diminished by the disordering effect of vortices and the scaling, which is perhaps due to a new renormalized trajectory, is only apparent. The true scaling regime associated with the O(3) [O(4)] fixed point will correspond to much larger correlation lengths than those studied. We believe that a similar effect caused the bogus signal for scaling in the analysis of the SO(4) matrix model [3] and the mismatch between the observed mass-gap and the Bethe-ansatz predictions.

We conclude that the RP^2 and O(3) spin models are in the same universality class and that there is no evidence to the contrary. This confirms the conclusions of Hasenbusch [8] and Niedermayer *et al.* [7], but is at variance with the proposition of Caracciolo *et al.* [2] that the continuum limits of these two models are distinct. These latter authors propose that there is a continuous set of universality classes in a 2D model with mixed isovector and isotensor O(3) spin interactions. The O(3) and RP^2 theories correspond to the pure isovector and pure isotensor interactions, respectively, and the proposition of Caracciolo *et al.* requires that these two models be in different universality classes. The work presented in this paper shows that the opposite is true and hence that the existence of a continuous set of universality classes in the mixed model is unlikely.

VII. CONCLUSIONS

In this paper we have studied the 2D RP^2 gauge model that is characterized by two couplings (β,μ), where μ is the chemical potential controlling the vorticity computed from the gauge field plaquette expectation value. We have found that the role played by the vorticity in the nature of the phase diagram is crucial. Using standard methods, we confirm the existence of a first-order transition (Figs. 5–7), first suggested by Solomon *et al.* [6], in the (β,μ) plane separating phases of high and low vorticity. The critical point terminating this first-order line is established to lie in the range $7.0<\beta_c<7.5$, $\mu_c\sim -0.26$, which implies the existence of a ''vorticity'' fixed point controlling the continuous transition at (β_c,μ_c). We use the Monte Carlo renormalization group for blocking the spin-spin interaction and plaquette expectation values $\langle A\rangle$ and $\langle P\rangle$ to investigate the topology of the

renormalization group flows. We verify the presence of the O(3)-renormalized trajectory (at $\mu=\infty$) and find results consistent with the known three-loop β function for sufficiently large β once the finite lattice-spacing artifact has been taken into account. We establish the existence of new scaling flows in the $(\langle A\rangle,\langle P\rangle)$ plane (Figs. 3 and 4) and conjecture that they are due either to the ghost of the Kosterlitz Thouless renormalized trajectory in the XY model or to a new renormalized trajectory and its associated fixed point, which should lie out of the (β,μ) plane in the complete space of couplings. The scaling flows are consistent with a critical exponent $\kappa\approx 4-5$, and the projection of the conjectured fixed point onto the (β,μ) plane is deduced to be in the range $\beta^*\approx 6.5-7.5$, $\mu^*\approx -0.31$ to -0.26. Although the values of (β_c,μ_c) and (β^*,μ^*) are very similar, there are strong arguments against identifying the conjectured fixed point with the ''vorticity'' fixed point. One is that the exponent κ is much larger than that expected at the ''vorticity'' fixed point, and another is that such an identification would imply a fixed point in the $(\langle A\rangle,\langle P\rangle)$ flows for bare couplings (β_c,μ_c), with a consequent divergence in certain correlation lengths. This is contradicted by the fact that, because of the presence of nonzero vorticity, these correlation lengths are bounded from above by the corresponding quantities in the O(3) model ($\mu=\infty$) at the same β, which are known not to diverge for $\beta<\infty$. A consequence is that the critical point at (β_c,μ_c) cannot be in the domain of attraction of the conjectured fixed point. The scaling flows dominate the flows in their vicinity and in particular give rise to a crossover (Figs. 6 and 7) between regions of high vorticity (lower β) and low vorticity (higher β) accompanied by a rapid increase in the correlation length as the disorder is reduced. We conclude that simulations in the neighborhood of the crossover region for $\mu>-0.26$ will show ''pseudo'' scaling [3] because of the proximity of these scaling flows. The true continuum limit for such models will not be observed until true scaling, controlled by the O(3) fixed point, has been established at larger β and very much larger correlation length. This is the case for the RP^2 spin model ($\mu=0$) whose continuum limit is controlled by the O(3) fixed point and which is thus in the same universality class as O(3), contradicting Caracciolo *et al.* [2], but confirming the work of Hasenbusch [8] and Niedermayer *et al.* [7]. It also gives an explanation for the results discussed by Caracciolo *et al.* [1]. In Fig. 10 an artist's impression of the renormalization group flows is given for one scenario consistent with our results. The natures of any new fixed points are not established because of the known difficulty [16] in distinguishing between fits of different scaling forms and the compatibility of the observed scaling with a second-order scaling form, given by Eq. (5.11), is of phenomenological significance only. It is quite possible that any fixed point whose existence we infer from the data is of Kosterlitz-Thouless type.

Our investigation has shown that the nature of gauged spin models is complicated and it is difficult to pin down more about the nature and location of the topological features of the renormalization group flows without more information concerning the relevant operators in each case. However, it is clear that a fixed point in a larger coupling constant space can be close enough to the subspace of simple models that it very strongly influences observables and the outcome of tests for scaling in exactly that region accessible by simulation, namely, for those couplings for which the correlation lengths have increased to the practical limit measurable on modern computers. This influence is strengthened if the exponent of the associated renormalized trajectory is large. The model studied in this paper is a good example of this effect.

It would be interesting to more accurately locate the critical point at (β_c,μ_c) terminating the first-order line and investigate the continuum limit it defines, and it may be that such a study could usefully employ an optimized blocking scheme and/or an improved action.

ACKNOWLEDGMENTS

This work was supported by NATO collaborative research Grant No. CRG950234 and DOE Grant Number DE-FG02-85ER40237. The authors wish to thank Ian Drummond for useful conversations. The computing resources were provided by the High Performance Computing Facility, University of Cambridge, and by the Computer Centre, University of Tokyo.

[1] S. Caracciolo *et al.*, Nucl. Phys. B (Proc. Suppl.) **30**, 815 (1993).
[2] S. Caracciolo *et al.*, Phys. Rev. Lett. **71**, 3906 (1993).
[3] M. Hasenbusch and R. R. Horgan, Phys. Rev. D **53**, 5075 (1996).
[4] T. Hollowood, Phys. Lett. B **329**, 450 (1994).
[5] M. Lüscher, P. Weisz, and U. Wolff, Nucl. Phys. **B359**, 221 (1991).
[6] S. Solomon *et al.*, Phys. Lett. **112B**, 373 (1982).
[7] F. Niedermayer *et al.*, Phys. Rev. D **53**, 5918 (1996).
[8] M. Hasenbusch, Phys. Rev. D **53**, 3445 (1996).
[9] B. Nienhuis and N. Nauenberg, Phys. Rev. Lett. **35**, 477 (1975).
[10] A. Hasenfratz and P. Hasenfratz, Nucl. Phys. **B295**, 1 (1988).
[11] A. P. Gottlob, M. Hasenbusch, and K. Pinn, Phys. Rev. D **54**, 1736 (1996).
[12] R. H. Swendsen, Phys. Rev. Lett. **52**, 2321 (1984).
[13] C. Lang and M. Salmhofer, Phys. Lett. B **205**, 329 (1988).
[14] J. Hoek, Nucl. Phys. **B329**, 240 (1990).
[15] A. Hoch and R. R. Horgan, Nucl. Phys. **B380**, 337 (1992).
[16] E. Seiler *et al.*, Nucl. Phys. **B305**, 623 (1988).
[17] W. Janke and K. Nather, Phys. Lett. A **157**, 11 (1991).
[18] H. Kunz and G. Zumbach, Phys. Rev. B **46**, 662 (1992).
[19] K. Huang and J. Polonyi, Int. J. Mod. Phys. A **6**, 409 (1991).